A Genetic Screen for Hedgehog Targets Involved in the Maintenance of the Drosophila Anteroposterior Compartment Boundary

Mátyás Végh and Konrad Basler[1]

Institut für Molekularbiologie, Universität Zürich, CH-8057 Zürich, Switzerland

Manuscript received November 7, 2002
Accepted for publication January 9, 2003

ABSTRACT

The development of multicellular organisms requires the establishment of cell populations with different adhesion properties. In Drosophila, a cell-segregation mechanism underlies the maintenance of the anterior (A) and posterior (P) compartments of the wing imaginal disc. Although *engrailed* (*en*) activity contributes to the specification of the differential cell affinity between A and P cells, recent evidence suggests that cell sorting depends largely on the transduction of the Hh signal in A cells. The activator form of Cubitus interruptus (Ci), a transcription factor mediating Hh signaling, defines anterior specificity, indicating that Hh-dependent cell sorting requires Hh target gene expression. However, the identity of the gene(s) contributing to distinct A and P cell affinities is unknown. Here, we report a genetic screen based on the *FRT/FLP* system to search for genes involved in the correct establishment of the anteroposterior compartment boundary. By using double *FRT* chromosomes in combination with a wing-specific *FLP* source we screened 250,000 mutagenized chromosomes. Several complementation groups affecting wing patterning have been isolated, including new alleles of most known Hh-signaling components. Among these, we identified a class of *patched* (*ptc*) alleles exhibiting a novel phenotype. These results demonstrate the value of our setup in the identification of genes involved in distinct wing-patterning processes.

DROSOPHILA limbs are subdivided into distinct sets of cells designated as compartments (Garcia-Bellido *et al.* 1973; Lawrence and Struhl 1996; Dahmann and Basler 1999). Once cells have been allocated to a particular compartment, they remain part of it throughout development. The boundary separating two adjacent compartments cannot be crossed by wild-type cells. Although other models have been discussed in the past, it is widely assumed that cells of opposite compartments are kept separate by distinct cell adhesion properties referred to as "cell affinities" (Garcia-Bellido 1975; Dahmann and Basler 1999).

The Drosophila wing is subdivided by two such lineage boundaries, one between the anterior (A) and posterior (P) compartments and another between the dorsal (D) and ventral (V) compartments. While it was originally assumed that compartment-specific properties are controlled in a compartment-wide manner by selector genes (Garcia-Bellido 1975), studies over the past 5 years have indicated a uni- or bidirectional interplay between cells of opposite compartments across the boundary. For example, cells on the dorsal and ventral sides of the D/V boundary express high levels of the Notch ligands Serrate and Delta, respectively. The resulting Notch signaling activity in cells flanking the D/V boundary contributes in an important, yet not entirely understood, manner to its maintenance.

At the A/P boundary, the signaling mechanisms that control compartment-specific adhesion properties are better understood. P cells heritably express the selector gene *engrailed* (*en*) (Lawrence and Morata 1976). En programs P cells to secrete Hedgehog (Hh) protein, which acts as a short-range signal on A cells located close to the compartment boundary (Basler and Struhl 1994). En also prevents the expression of the Hh signal transduction component Cubitus interruptus (Ci) in P cells. Hence, only A cells can respond to Hh, and they do so by upregulating the expression of Hh target genes, such as *decapentaplegic* (*dpp*) and *patched* (*ptc*). *dpp* encodes a BMP homolog that functions as a long-range morphogen to establish different cell fates along the anteroposterior axis. *ptc* encodes the receptor for Hh and negatively regulates the signaling activity of Smoothened (Smo). Upregulation of Ptc levels in response to the Hh signal promotes the sequestration of Hh protein, thereby reducing the range of Hh activity to a narrow stripe of A cells (Chen and Struhl 1996). Clonal analysis has demonstrated a crucial role for both the selector gene *en* and the Hh signal transduction components in defining compartment-specific cell affinities. For example, if A cells adjacent to the boundary become mutant for *smo* (Blair and Ralston 1997; Rodriguez and Basler 1997), they sort out from other A cells and segregate into P territory. Thus the Hh signal induces in A cells an important aspect of the compartmental cell

[1]*Corresponding author:* Institute for Molecular Biology, University of Zürich, Winterthurerstrasse 190, CH-8057 Zürich, Switzerland. E-mail: basler@molbio.unizh.ch

segregation system. Cells lacking both *en* and *ci* functions sort out from cells of both compartments (Dahmann and Basler 2000). This suggests that the cell adhesion properties of P and A cells close to the boundary depend on the activity of En and the response to Hh, respectively. The requirement of the zinc-finger protein Ci for establishing A-specific cell segregation properties indicates that putative cell adhesion molecules are regulated transcriptionally (Dahmann and Basler 2000).

In this study we present a genetic screen designed to identify genes required for the maintenance of the A/P compartment boundary. On the basis of the assumption that mutations in such genes would cause phenotypes similar to those observed with mutations in *smo* or *ci*, we established a wing-specific, F_1, FRT-FLP screen to create clones of wing cells carrying random mutations (Golic 1991; Xu and Rubin 1993). Wing specificity was achieved by driving the expression of *flp* with regulatory elements of the *vestigial* (*vg*) gene. Efficient coverage of the genome was achieved by the use of "double FRT chromosomes," which carry an FRT sequence on both sides of an autosomal centromere. Approximately 250,000 mutant chromosomes were analyzed. Despite the high number of *smo*-like mutations found, no gene encoding a novel cell adhesion molecule was identified. However, one complementation group that exhibits a strong *smo*-like phenotype was identified as a class of gain-of-function *ptc* alleles that provide new insights into the action of the Hh ligand and receptor. Moreover, we demonstrate that the screen is ideally suited to identifying genes controlling wing patterning.

MATERIALS AND METHODS

Drosophila genotypes: We tested the following *gal4/UAS-flp* combinations for their range of activity (Figure 2):

dpp::flp: *y w*; P[mini w^+, *dpp-gal4*] P[mini w^+, *UAS-flp*]/TM6b;
ptc::flp: *y w*; P[mini w^+, *UAS-flp*] P[mini w^+, *gal4*]*ptc*/TM6b;
spalt::flp: *y w*; P[mini w^+, *spalt-gal4*] P[mini w^+, *UAS-flp*]/TM6b;
vg::flp: *y w*; P[mini w^+, *gal4*]*vgBE* P[mini w^+, *UAS-flp*]/CyO.

These combinations were crossed to *y w*; *actin5C*-FRT-*Draf*-stop-FRT-*lacZ*/CyO flies. Third instar imaginal disc staining of β-galactosidase (β-Gal) was carried out according to standard procedures.

For generating interchromosomal recombination on the X chromosome, the following genotype was generated: *y w* P[y^+, *hsp70*-HA-*gfp*-HA] P[ry^+, *hsp70-neo*, FRT]19/*y w* P[ry^+, *hsp70-neo*, FRT]19; P[mini w^+, *gal4*]*vgBE* P[mini w^+, *UAS-flp*]/CyO.

We tested the following *gal4/UAS-flp* combinations for generating *smo* mutant clones (Figure 1):

with *hsp70-flp*: *y w*; P[ry^+, *hsp70-flp*]; smo^3 P[mini w^+, FRT]39/P[ry^+, *hsp70-flp*]; P[y^+, *hsp70-cd2*] P[mini w^+, FRT]39;
with *dpp::flp*: *y w*; P[ry^+, *hsp70-flp*]; smo^3 P[mini w^+, FRT]39/P[y^+, *hsp70-cd2*] P[mini w^+, FRT]39; P[mini w^+, *dpp-gal4*] P[mini w^+, *UAS-flp*]/TM6b;
with *spalt::flp*: y w; P[ry^+, *hsp70-flp*]; smo^3 P[mini w^+, FRT]39/P[y^+, *hsp70-cd2*] P[mini w^+, FRT]39; P[mini w^+, *spalt*-Gal4] P[mini w^+, *UAS-flp*]/TM6b;
with *ptc::flp*: y w; P[ry^+, *hsp70-flp*]; smo^3, P[mini w^+, FRT]39/P[y^+, *hsp70-cd2*] P[mini w^+, FRT]39; P[mini w^+, Gal4]*ptc*; P[mini w^+, *UAS-flp*]/TM6b;
with *vg::flp*: *y w* ; smo^3, P[mini w^+, *gal4*]*vgBE* P[mini w^+, FRT]39/P[y^+, *hsp70-cd2*] P[mini w^+, FRT]39; P[mini w^+, *UAS-flp*]/TM6b.

2xFRTs: 2xFRTs were generated by combination of the corresponding single FRTs through meiotic recombination. To test the efficiency of the 2xFRTs in combination with the *vg::flp*, markers for clonal analysis were recombined onto 2xFRTs, resulting in the following genotypes:

for the second chromosome: *y w hsp70*-flp; P[mini w^+, *gal4*]*vgBE* P[mini w^+, *UAS-flp*] P[ry^+, *hsp70-neo*, FRT]40 P[ry^+, *hsp70-neo*, FRT]42/P[mini w^+, arm-*lacZ*) P[ry^+, *hsp70-neo*, FRT]40 P[ry^+, *hsp70-neo*, FRT]42 P[mini w^+, *hsp70*-HA-*gfp*, smo^+];
for the third chromosome: *y w hsp70-flp*; P[mini w^+, *gal4*]*vgBE* P[mini w^+, *UAS-flp*]; P[y^+, *hsp70-cd2*] P[mini w^+, FRT]79 P[ry^+, *hsp70-neo*, FRT]82 P[mini w^+, *hsp70*-HA-*gfp*, smo^+].

Clonal analysis of new ptc alleles (Figure 6): For the analysis of homozygous mutant clones in wing imaginal discs, flies of the following genotypes were generated:

for observation of compartmental segregation behavior: *y w hsp70-flp*; P[ry^+, *hsp70-neo*, FRT]42 P[y^+, *hsp70-cd2*] P[mini w^+, *lacZ*]*hh*/P[ry^+, *hsp70-neo*, FRT]40 P[ry^+, *hsp70-neo*, FRT]42 ptc^{N15};
for effect on Hh target genes: *y w hsp70-flp*; P[mini w^+, *lacZ*]*dpp* P[ry^+, *hsp70-neo*, FRT]42 P[y^+, *hsp70-cd2*]/P[ry^+, *hsp70-neo*, FRT]40 P[ry^+, *hsp70-neo*, FRT]42 ptc^{N15}.

Overexpression of Ptc (Figure 7): For overexpression analysis of mutant and wild-type *ptc* alleles, we tested the following *gal4/UAS-ptc* combinations:

with *en-gal4*:

y w; P[mini w^+, *lacZ*]*ptc* P[mini w^+, *gal4*]*en*/P[mini w^+, *UAS-*ptc^{wt}*-myc*];
y w; P[mini w^+, *lacZ*]*ptc* P[mini w^+, *gal4*]*en*/P[mini w^+, *UAS-*ptc^{mut}*-myc*];

with *apt-gal4*:

y w; P[mini w^+, *lacZ*]*ptc* P[mini w^+, *gal4*]*apt*/P[mini w^+, *UAS-*ptc^{wt}*-myc*];
y w; P[mini w^+, *lacZ*]*ptc* P[mini w^+, *gal4*]*apt*/P[mini w^+, *UAS-*ptc^{mut}*-myc*].

Mutagenesis: Males isogenic for the corresponding FRT chromosome were fed a 25-mM ethyl methanesulfonate (EMS), 1% sucrose solution. Mutagenized males were then mated in a 1:4 ratio to the tester virgins. The F_1 progeny were scored using a stereomicroscope for alteration of wing patterning. Flies exhibiting an interesting phenotype were backcrossed to the tester stock for a rescreen to check for germline transmission and reproducibility of the mutation. If possible, several phenotypic males were then mated to a balancer stock to establish a stable mutant line. Scoring F_1 progeny and the rescreen was different in the screen for the X chromosome. Here, only F_1 females could be scored and five individual stocks of every mutation were set up from single phenotypic virgins. Out of these five individual stocks one was selected on the basis of male lethality or the presence of viable males exhibiting a phenotype and by reproducibility of the phenotype when crossed to *vg::flp*. The genotypes of the mutagenized males were as follows: *y w* P[y^+, *hsp70-gfp*] P[ry^+, *hsp70-neo*, FRT]19/Y for the X chromosome; *y w hsp70-flp*; P[ry^+, *hsp70-neo*, FRT]40 P[ry^+, *hsp70-neo*, FRT]42 P[y^+] for the second chromosome; and *y w hsp70-flp*; P[mini w^+, FRT]79 P[ry^+, *hsp70-neo*, FRT]82 P[y^+] for the third chromosome. The tester

stocks that were crossed to the mutagenized males and used for rescreening were *y w* P[*ry*$^+$, *hsp70-neo*, FRT]19; P[mini *w*$^+$, *gal4*]*vgBE* P[mini *w*$^+$, *UAS-flp*] for the X chromosome; to *y w hsp70-flp*; P[mini *w*$^+$, *gal4*]*vgBE* P[mini *w*$^+$, *UAS-flp*] P[*ry*$^+$, *hsp70-neo*, FRT]40 P[*ry*$^+$, *hsp70-neo*, FRT]42 for the second; and *y w hsp70-flp*; P[mini *w*$^+$, Gal4]*vgBE* P[mini *w*$^+$, *UAS*-flp] P[mini *w*$^+$, FRT]79 P[*ry*$^+$, *hsp70-neo*, FRT]82 for the third chromosome. The following stocks were used for balancing: FM7 for mutations on the X and *y w hsp70-flp*; CyO/Sp and *y w hsp70-flp*; TM6b/MKRS for second and third chromosomal mutations.

Mapping of mutations: Mutations on the second and third chromosome were first mapped to one chromosomal arm by reproducing the phenotype with single FRT chromosomes. Mutations conferring similar phenotypes and mapping to the same chromosomal arm were then grouped by complementation analysis. Complementation groups exhibiting a known phenotype were tested for complementation of known null alleles of the candidate gene. The alleles used in this study were as follows: *smo*^{3}, a null allele of *smo*; *fu*^{A}, a kinase dead allele of *fu*; *col*^{1}, an amorphic allele of *collier/knot*; *ptc*^{IIW}, a null allele of *ptc*; Df(2R)enE, a deficiency that removes *en* and the closely related *invected* (*inv*) gene; *pka-C1*^{E95}, a null allele for the catalytic subunit of protein kinase A; and *cos2*^{5}, a null allele of *costal-2*. Other mutations were mapped by using the Bloomington deficiency kit.

Immunohistochemistry: Imaginal discs dissected from late third instar larvae were fixed and stained with the appropriate antibodies to mark clones and monitor reporter and transgene expression, respectively. If required, a heat shock for 1 hr at 38° followed by a recovery for 1 hr at 25° was given to have clonal marker genes expressed. Antibodies were rabbit polyclonal anti-green fluorescent protein (GFP; CLONTECH, Palo Alto, CA), mouse monoclonal anti-β-Gal (Cappel), mouse monoclonal anti-Myc 9E10, and Alexa 488 and 594 secondary antibodies (Molecular Probes, Eugene, OR).

Construction of *UAS-ptc*: Ptc cDNA derived from an available *UAS-ptc* construct (Johnson *et al.* 2000) was N-terminally fused with an *myc* epitope and reinserted into a pUAST vector. For generation of mutated *ptc*, site-directed mutagenesis was performed using the QuikChange site-directed mutagenesis kit (Stratagene, La Jolla, CA). The construct presented here contains two missense mutations producing a protein with both R111W and G276D amino acid exchanges in the first extracellular loop.

RESULTS

***smo* mutant clones cause characteristic defects in the venation and bristle pattern of the wing:** *smo* mutant cell clones located along the A/P compartment boundary position themselves in P territory even if they originate from A compartment cells (Blair and Ralston 1997; Rodriguez and Basler 1997). Apparently, the transduction of the Hh signal programs Hh-receiving cells to sort out from cells not transducing Hh, be these wild-type P cells that lack Ci or experimental A cells mutant for *smo*. Mutations in genes encoding essential mediators or effectors of this Hh-induced segregation behavior should cause similar phenotypes; *i.e.*, mutant A clones should also enter posterior territory. The situation in which such clone behavior can best be observed is fixed preparations of third instar imaginal discs in which the clones and the position of the A/P boundary are independently marked (Blair and Ralston 1997; Rodriguez and Basler 1997). This assay is not suitable, however, for a high-throughput screen. We searched therefore for a reliable adult phenotype that is caused by the sorting-out phenomenon of *smo* mutant boundary cells.

Due to the maintenance of some A compartment properties, *smo* mutant clones originating from anterior cells can affect the pattern of the third (L3) and fourth (L4) longitudinal veins as well as the identity of wing margin bristles (Blair and Ralston 1997; Rodriguez and Basler 1997; Figure 1, B–D). We observed that L4 was often disrupted, or partially duplicated, and shifted posteriorly. In addition, double-row wing margin bristles, typically present at the wing margin between L2 and L3, occasionally reappear more posteriorly. In some cases, even completely anteriorized wings could be observed (see also Chen and Struhl 1996). Often, ectopic veins between L3 and L4 were detected in conjunction with small duplications of L3. L3 is formed in A cells that are positioned next to Hh-receiving cells (Biehs *et al.* 1998). *smo* mutant clones that are not in immediate contact with P cells do not move into P territory. Instead, they form ectopic boundaries of Hh target gene expression, which consequently result in ectopic or defective L3 veins.

We concluded therefore that a screen for mutations affecting vein L4 or posterior wing margin bristles should lead to the identification of genes coding for Hh signal transduction components or downstream effectors responsible for the Hh-dependent A/P cell segregation system.

The *vg::flp* system induces recombination specifically in the wing: To set up a wing-specific F_1 screen we sought to modify the commonly used FRT-FLP system (Golic 1991; Xu and Rubin 1993). In most previous cases FLP is driven by a heat-shock-inducible promoter that is transiently activated at a particular time during development. However, without spatially controlling the expression of the FLP recombinase, clones may be absent in the tissue of interest, or even worse, clones may be present in other tissues where they can be harmful. The latter problem is of particular concern for an F_1 screen, as an individual exhibiting the desired phenotype has to be propagated to recover the underlying mutation.

Following the approach chosen by Newsome *et al.* (2000) who expressed FLP in an eye-specific manner by using the *eyeless* enhancer, we tested four enhancers [*ptc*, *dpp*, *spalt*, and *vg boundary enhancer* (*vgBE*)] for their ability to drive high levels of FLP expression in the wing. *ptc* and *dpp* are both Hh target genes, so their enhancers are active in a stripe of A cells along the anteroposterior compartment boundary, *i.e.*, in the region critical for A affinity (Figure 2A). In contrast, the enhancer of the Dpp target gene *spalt* is active in a broader stripe centered on the *ptc/dpp* stripe and comprising both A and P cells (Lecuit *et al.* 1996; Nellen *et al.* 1996; Figure 2B).

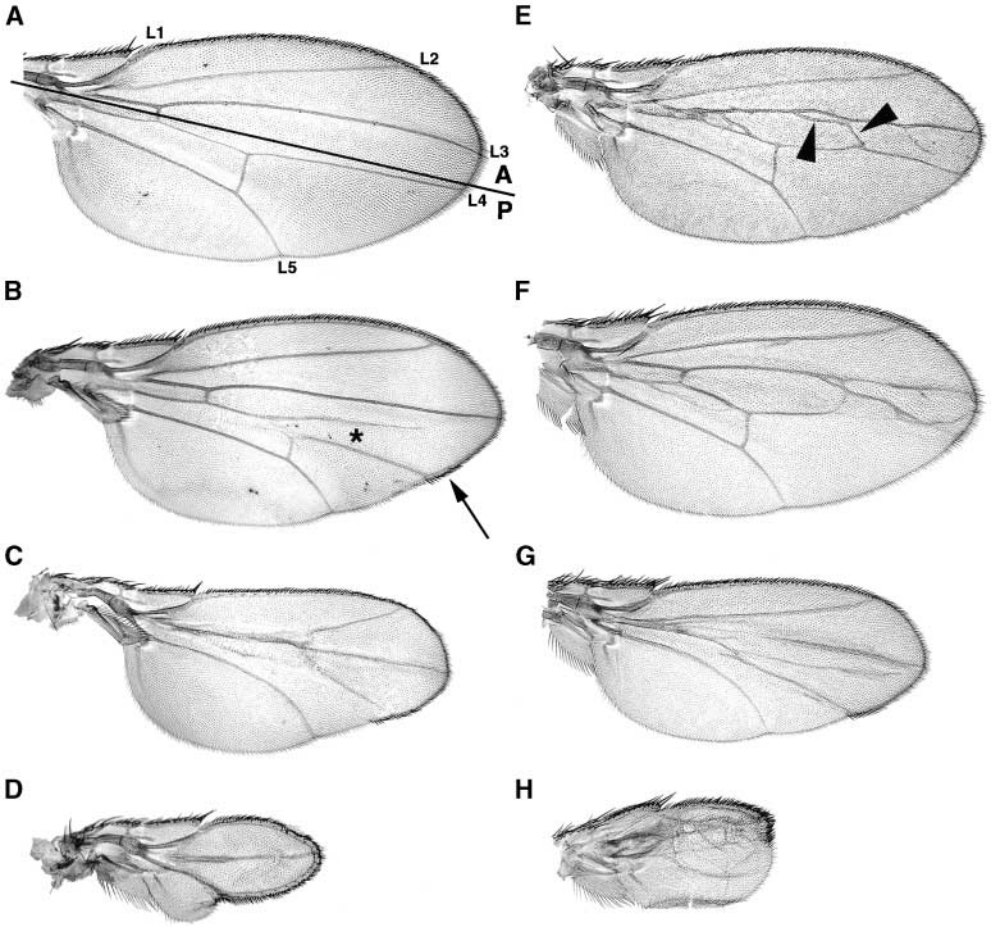

Figure 1.—Drosophila wings with *smo* mutant clones induced by means of different *flp* transgenes. (A) Wild-type wing for comparison with the longitudinal veins designated as L1–L5 and the A/P compartment boundary represented by the solid line. (B–D) When clones have been induced by the use of a heat-shock-driven *hsp70-flp* transgene, the adult wings exhibit different penetrance of a phenotype that can be correlated with the sorting out of *smo* mutant clones: duplication and displacement of L4 (marked by the asterisk in B) and the reappearance of anterior margin bristles in a more posterior margin region (indicated by the arrow in B); more severe phenotypes display an increasing anteriorization of the wing (C and D). (E) A wing where *UAS-flp* was driven by *dpp-gal4*. Ectopic veins between L3 and L4 are indicated by arrowheads. When *spalt-gal4* or *ptc-gal4* was used instead, the phenotype was very similar (data not shown). (F–H) Wings of flies with the *vgBE-gal4 UAS-flp* combination.

Thus the *spalt* enhancer in addition would permit the generation of mutant P clones potentially moving into A territory. The fourth candidate, the *vestigial* D/V boundary enhancer, is activated by the Notch-Su(H) pathway and is thus entirely independent of Hh signaling (Kim *et al.* 1996). In the wing pouch of third instar larvae, this enhancer drives expression in a thin stripe along the dorsoventral compartment boundary corresponding to the presumptive wing margin cells (Figure 2D). Thus, the relevant region of activity for our screen would be the distal tip of the wing where the anteroposterior and dorsoventral axes intersect.

As we have previously observed that high levels of FLP recombinase are required for interchromosomal recombination, we used the Gal4 system to amplify the activities of the above-mentioned enhancers. Each of the four corresponding Gal4 drivers were used in combination with a *UAS-flp* transgene to induce *smo* mutant clones. *ptc*, *dpp*, and *spalt-gal4* all caused very similar wing phenotypes with ectopic veins appearing between L3 and L4 (arrowheads in Figure 1E), but no displacement of L4 or defects of the bristle pattern was observed. Examination of third instar imaginal discs of such animals revealed that the *smo* clones were small and probably arose late in development (data not shown). Despite the rather mild wing phenotypes, animals with the *ptc-gal4* and *dpp-gal4* transgenes exhibited further defects on thorax, head, and legs that weakened these flies significantly.

In contrast to the above-described genotypes, the *vgBE-gal4 UAS-flp* combination (hereafter called *vg::flp*) was expected to generate *smo* clones only at the distal tip of the wing. However, a wide variety of adult wing phenotypes was observed, very similar to those associated with smo clones generated by a heat-shock-induced *hsp70-flp* transgene (Figure 1, F–H). Moreover, despite the severe disruption of wing pattern, these flies were fully viable and did not exhibit defects in other tissues. The severity of the wing phenotype, however, was unexpected since the *vgBE* enhancer shows a spatially restricted expression pattern during third instar. To test whether this enhancer drives *flp* expression elsewhere at earlier stages we used an *actin5c* > *stop* > *lacZ* transgene to irreversibly mark cells experiencing FLP activity. A *UAS-lacZ* transgene was used as a control to monitor the current state of Gal4, and thus FLP, activity. Whereas wings and halteres of the control animals showed a thin *lacZ*-expressing stripe along the dorsoventral boundary (Figure 2D), the *actin5c* > *stop* > *lacZ* animals exhibit β-Gal activity in the entire wing disc (Figure 2C). To confirm and extend this observation we also tested whether interchromosomal recombination occurs throughout the

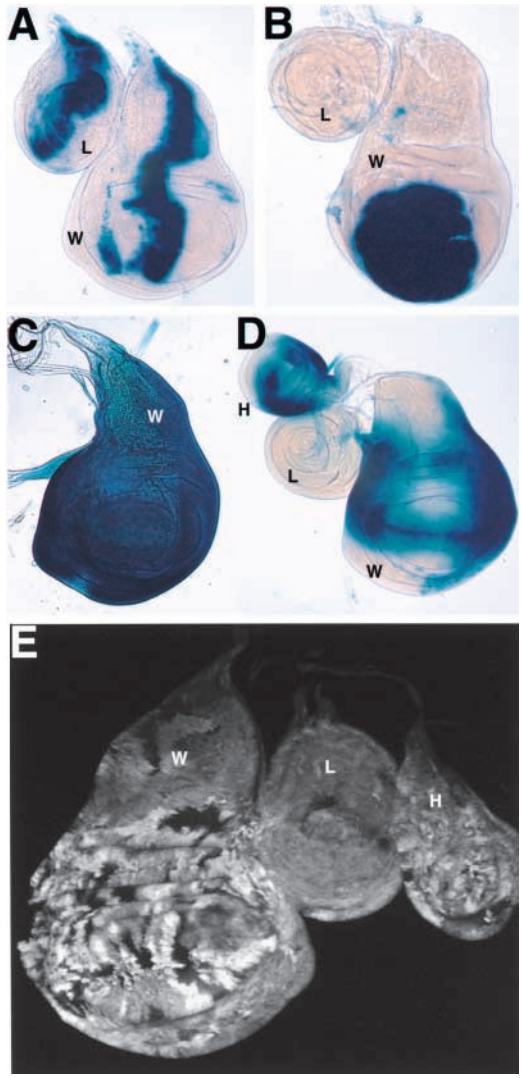

FIGURE 2.—*vgBE-gal4* is active in almost all cells of the wing and haltere primordia during larval development. β-Gal staining was performed on wing (W), leg (L), and haltere (H) discs of the following genotypes: (A) *ptc-gal4 UAS-flp/ actin5C*-promoter-FRT-*Draf-stop*-FRT-*lacZ*; (B) *spalt-gal4 UAS-flp/ actin5C*-promoter-FRT-*Draf-stop*-FRT-*lacZ*; (C) *vgBE-gal4 UAS-flp/ actin5C*-promoter-FRT-*Draf-stop*-FRT-*lacZ*; and (D) *vgBE-gal4 UAS-flp/ UAS-lacZ*. (E) GFP expression in imaginal discs of the genotype *hsp70-gfp* FRT19/FRT19; *vgBE-gal4 UAS-flp*. Discs of the genotype *dpp-gal4 UAS-flp/ actin5C > Draf > lacZ* had a similar *lacZ* pattern in the wing as those in A (not shown).

wing primordium with *vg::flp* and used an X chromosomal FRT with a *hsp70-gfp* reporter to mark such clones. Again we observed recombination to occur throughout the entire wing disc (Figure 2E). Moreover, the size of the clones suggests that many of them were induced at early larval stages, which is in accordance with the strong *smo* phenotypes observed with *vg::flp*. We conclude from these experiments that all cells of the wing and haltere discs, but not those of other discs, must exhibit an early transient *vgBE* enhancer activity. For these reasons the *vg::flp system* was considered to be the most suitable source of recombinase for our purpose.

The use of 2xFRTs to screen entire autosomes: A major disadvantage of FRT screens is that only a small fraction of the genome can be screened at once, *i.e.*, one chromosomal arm. In an attempt to overcome this drawback we used meiotic recombination to construct chromosomes with FRTs on both sides of the centromere (referred to as 2xFRTs). We tested their use by combining them with *vg::flp* and appropriate imaginal disc marker genes. For both the second (Figure 3B) and third (Figure 3C) autosomal 2xFRTs, we observed efficient and independent recombination on both sides of the centromere. Importantly, no significant preference of one FRT over the other could be detected. In theory, exchange of chromosomal arms can occur as long as recombinase is present. Continuous supply of recombinase eventually approaches a state of complete loss of heterozygous cells and a concomitant presence of homozygous cells, *i.e.*, "twinspots" and "clones" (Figure 3A). In the case of the first and third chromosomes, this state was nearly reached. However, since the *vg::flp* components are located on the left arm of the second chromosome, recombination of this arm can result in daughter cells that have lost the recombinase and are therefore no longer able to exchange the right arms of the second chromosome. Hence, they will remain heterozygous for the right arm if no recombination event has occurred there previously. Even though such cases were indeed found, we observed a high efficiency of clone induction for both arms of the second chromosome. We conclude from these experiments that the combination of 2xFRTs and *vg::flp* is ideally suited for a high-throughput F_1 screen for genes required for the segregation of A and P cells in the wing.

Identification of mutations conferring *smo*-like phenotypes: The 2xFRT chromosomes were mutagenized in males with EMS and crossed to *vg::flp* females with the corresponding 2xFRTs (Figure 4A). Approximately 100,000 mutant F_1 animals were screened for each autosome and 50,000 for the X chromosome (Table 1). Adults with interesting phenotypes were individually backcrossed to *vg::flp* flies to assess the reproducibility of the phenotype. In many cases the observed phenotype did not recur in the F_2 generation. However, many mutations did breed through, in which case several males displaying the same phenotype were then used to establish a balanced stock. The genetic setup for the X chromosome mutagenesis was complicated by the fact that clones could be generated only in females, and mutant females were required to establish stable, balanced stocks (see MATERIALS AND METHODS; Figure 4B). Finally, balanced stocks of second and third chromosome mutants were retested with 1xFRT chromosomes to assign the mutations to single chromosomal arms. Mutations exhibiting similar phenotypes and mapping to the same chromosomal arm were grouped and subjected to complementation analysis. Some complementation groups were then further mapped by noncom-

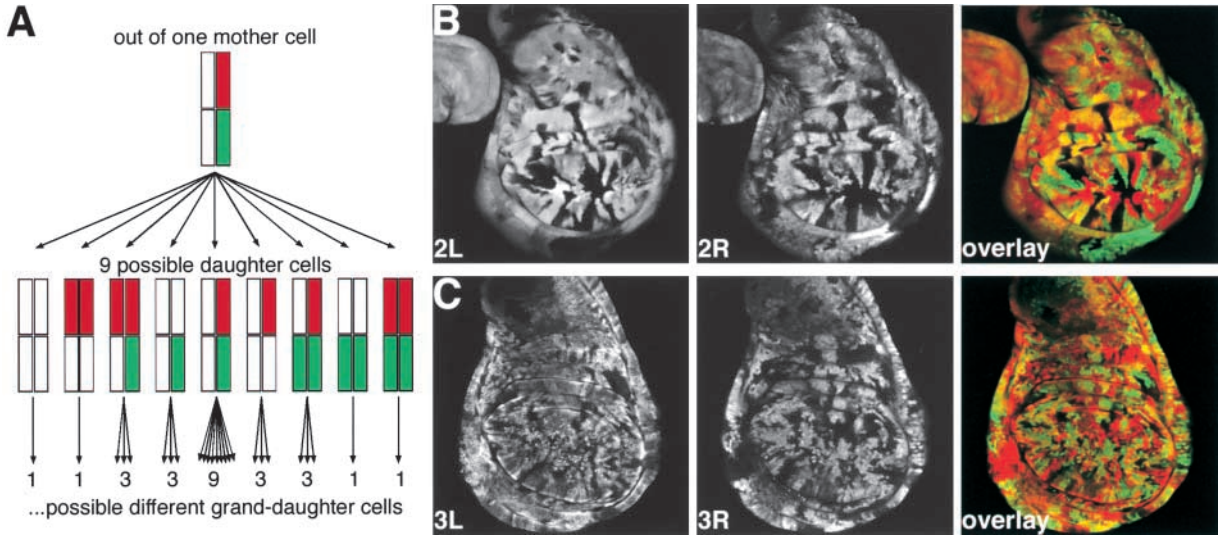

FIGURE 3.—2xFRTs allow the generation of clones with both chromosomal arms. (A) Schematic representation of the recombination events with a 2xFRT: the mother cell in the model is heterozygous for the red marker on one arm and the green marker on the opposite arm. Recombination can lead to nine genetically different daughter cells, depending on which chromosomal arm FLP-induced recombination occurred and which combination of chromosomal arms was paired together. If recombination and pairing resulted in a daughter cell identical to its mother cell, then another nine possible granddaughter cells could be created in the next round of recombination. However, if the daughter cell became homozygous for one arm, only recombination of the other still-heterozygous arm leads to different granddaughter cells. Daughter cells homozygous for both arms result in a recombinatorial dead end. Recombination in such cells no longer creates genetic diversity. Therefore, continuous supply of recombinase would promote the generation of homozygous cells. The combination of *vg::flp* with the 2xFRTs induces clones efficiently and independently on both left (2L and 3L) and right (2R and 3R) chromosomal arms for the second (B) and the third chromosome (C; see MATERIALS AND METHODS for the genotypes).

plementation of deficiencies or candidate genes (see MATERIALS AND METHODS).

Four complementation groups that exhibit *smo*-like phenotypes were identified (Table 2 and Figure 5, A–E and H). Whereas the first and fourth of these complementation groups exhibited defects representing the entire spectrum of *smo*-like phenotypes (Figure 5, A and E), the other two did not show any alterations in L4 and margin bristles but displayed ectopic veins between L3 and L4 and a partial or complete fusion of these two longitudinal veins (Figure 5, B–D). Complementation analysis with a *smo* null allele revealed that the first group represents new alleles of *smo* itself, supporting the validity of the screen. The second and third complementation groups were identified as new alleles of *collier* and *fused*. *collier*, also known as *knot*, is a Hh target gene encoding a transcription factor required for the formation of the L3/L4 intervein region (VERVOORT *et al.* 1999). Fused is a serine/threonine kinase that acts positively in Hh receiving cells (PREAT *et al.* 1990). The fourth complementation group behaved like the first, yet mapped to the right arm of the second chromosome and could therefore not be allelic to *smo*. To test whether this gene was involved directly in compartmental affinity or whether it functioned in Hh signal transduction, we examined mutant clones in wing imaginal discs for their sorting-out behavior and for alterations of Hh target gene expression, respectively. Consistent with the adult wing phenotype, mutant clones did indeed sort out into P territory (Figure 6A).However, mutant clones also failed to upregulate the Hh target gene *dpp* (Figure 6B). Hence, the new complementation group appeared to identify a locus required for the transduction of the Hh signal and was further analyzed as described below.

In addition to the above-described complementation groups, we isolated a further single mutation that caused an L4 phenotype. Surprisingly, analysis in discs revealed that mutant clones migrated from the P to the A compartment (data not shown). In agreement with this observation we found, however, that the mutation failed to complement a small deficiency removing the two neighboring genes *en* and *inv* and hence represents an allele of one of these two genes.

A new class of *ptc* alleles with properties of *smo* loss-of-function mutations: We focused our attention on the fourth complementation group. Apart from *smo*, only two other genes are known to be positive regulators of Hh signal transduction in the Hh receiving cells, *fu* and *ci*. Since *fu* is on the X and *ci* on the fourth chromosome, they could be excluded as candidate genes. We identified a deficiency, Df(2R)44CE, which failed to fully complement these new alleles (Table 3). Intriguingly, this deficiency is deleted for the *ptc* gene. Clones lacking *ptc* function display a gain rather than a loss of Hh signaling, rendering it unlikely that the new complementation group represented *ptc* alleles. However, since Ptc re-

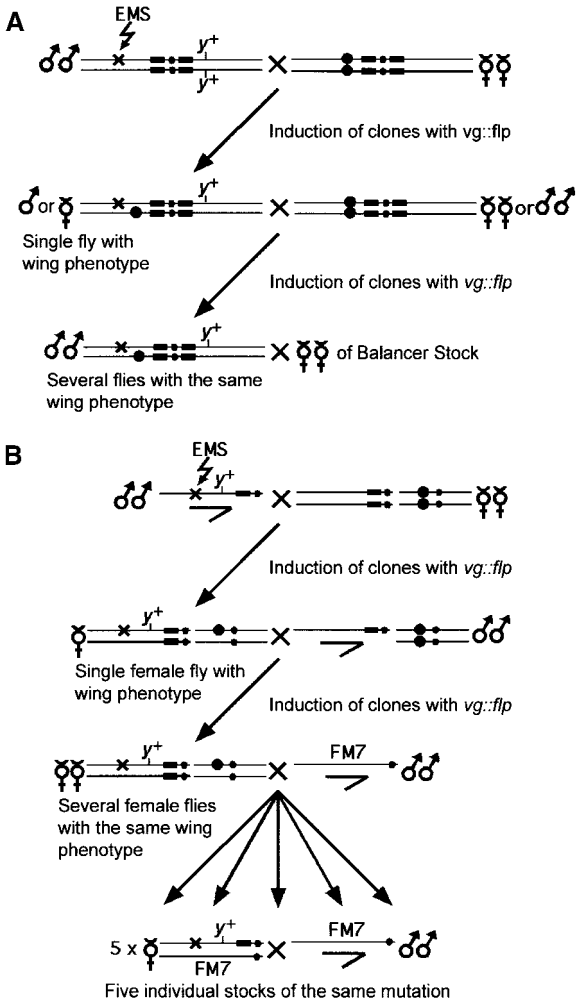

FIGURE 4.—Crossing schemes for the screen on the X and second chromosome. (A) Screening of the second and third chromosomes was basically identical except that *vg::flp*, which is located on the second chromosome, had to be recombined on the second 2xFRT chromosome of the tester flies. (B) In contrast to the autosomes, recombination of the X chromosome occurs only in females. As females can lose a mutation through meiotic recombination, five independent balanced lines of each mutation were established. One of these five lines was then selected on the basis of male lethality and reproducibility of the initially observed phenotype. FRT, rectangle; centromere, small solid circle; *vg::flp*, large solid circle; *yellow* + transgene, *y*+; and mutation, a cross.

presses Smo function upon Hh binding, it is possible that the new complementation group coded for Ptc proteins that can no longer be repressed by Hh and therefore would display *smo*-like phenotypes. To investigate this possibility, we tested those putative new *ptc* alleles for complementation of an additional deficiency, Df(2R)H3D3, and of two known *ptc* alleles, ptc^{IIW} and ptc^{S2} (Table 3 and Figure 6, C–F). All three new alleles fully complemented ptc^{S2}. ptc^{S2} carries a missense mutation in the sterol-sensing domain of Ptc and encodes a protein that can bind and sequester Hh, but is unable to repress Smo (CHEN and STRUHL 1998; MARTIN *et al.* 2001; STRUTT *et al.* 2001). None of the three new alleles, however, was fully viable over the protein null allele ptc^{IIW}. Rare escapers with such a genotype often exhibited a fusion of L3 and L4, similar to the *fused* phenotype (Figure 6D).

TABLE 1

Overview of the *vg::flp* screen

Chromosome	Screened F_1	Mutations scored	Stocks balanced
X	52,000	253	36
II	114,000	597	163
III	113,000	441	34

Synopsis of the screen. For the autosomes, both the female and male mutant F_1 progeny were screened, whereas for the X chromosome, only the female F_1 progeny could be taken into account. The reduction of balanced stocks *vs.* mutations scored was due to extinction or sterility of mutant F_1 animals or because the phenotype observed in F_1 animals was not reproduced in the rescreen.

To determine unambiguously whether the new alleles form a novel class of *ptc* alleles, we sequenced the entire *ptc* locus of all three mutants and identified missense mutations in all three alleles. Two mutations mapped to the first of the two large extracellular loops, R111W in ptc^{P83} and G276D in ptc^{N15}, while the third (N936Y in ptc^{Q67}) mapped to the second such loop. The three alleles differed in strength. According to their viability over the deficiency or over the *ptc* null allele, they could be ranked as $ptc^{N15} > ptc^{P83} > ptc^{Q67}$ with ptc^{N15} being the strongest allele.

The molecular nature and the clonal phenotype of these new *ptc* alleles suggested that the receptors encoded by these alleles cannot be repressed by the Hh ligand. To test the ability of the three mutant Ptc proteins to sequester Hh protein, we introduced their mutations into *UAS-ptc* transgenes. Wild-type or mutant *ptc* was then ectopically expressed in P compartment cells with an *en-gal4* driver, and Hh signaling was monitored with a *ptc-lacZ* reporter. While the wild-type *ptc* transgene caused a strong reduction or even ablation of *ptc-lacZ* expression (Figure 7A), presumably by sequestration of Hh protein, Hh signaling was unaffected by the expression of the mutant Ptc proteins (Figure 7B). To verify the functionality of the mutant *ptc* constructs, wild-type and mutant *ptc* transgenes were expressed in dorsal compartment cells using *apterous-gal4*. Both wild-type (Figure 7C) and mutant (Figure 7D) Ptc completely repressed Hh signaling in the dorsal compartment. To verify that the failure to sequester Hh was not due to a mislocalization of the mutant Ptc proteins, these proteins were localized *in situ* with respect to E-cadherin. No differences could be detected between the staining patterns of wild-type *vs.* mutant forms of Ptc (Figure 7, E and F). We conclude therefore that these novel mutant Ptc

TABLE 2

Complementation groups with *smo*-like wing-patterning defects

Name	Chromosome/ cytology	No. of alleles	Phenotype
smo	II/21B5-6	17	Disruption and duplication of L4, margin bristle defects
col	II/51C2-5	10	Ectopic veins between L3 and L4, fusion of L3 and L4
fu	X/17C5-7	9	Fusion of L3 and L4
ptc	II/44D2-5	3	Disruption and duplication of L4, margin bristle defects
en/inv	II/48A1-3	1	Disruption of L4

Five complementation groups exhibit complete or partial *smo*-like phenotypes. Cytology was determined by complementation analysis with deficiencies and known alleles of the corresponding gene.

proteins are not repressed by Hh because they fail to bind Hh efficiently, and they therefore inactivate Smo constitutively.

After completion of these studies a gain-of-function allele of *ptc*, ptc^{con}, was reported to also complement ptc^{S2} (Martin *et al.* 2001). This allele leads to an amino acid exchange in the first extracellular loop and hence is equivalent to the above-described class of *ptc* alleles.

Other mutations affecting wing patterning: In addition to the *smo*-like phenotypes we also scored a number of other phenotypes. A selection of mutants of these other phenotypic groups were kept for further analysis (Figure 5 and Table 4). Some of these were found to affect loci encoding negative regulators of Hh signaling, such as *pka* (Figure 5F), *cos2*, and *ptc* (Figure 5G). Others included negative modulators of other signaling pathways, such as *brk* (Figure 5I) and *sgg* (Figure 5K). The categories of observed phenotypes covered a wide range: notches, excessive or broadened veins, ectopic veins or loss of veins (Figure 5M), displaced or duplicated veins, blisters, bent wings, narrower or broader wings, smaller or larger wings, loss of margin bristles or ectopic margin bristles, axis duplications, ectopic bristles covering the wing blade or along veins (Figure 5O), hinge to wing transformations, crumpled wings, deformed compartments (Figure 5N), and outgrowths. The number and diversity of observed phenotypes validate the approach of a wing-specific FRT/FLP screen.

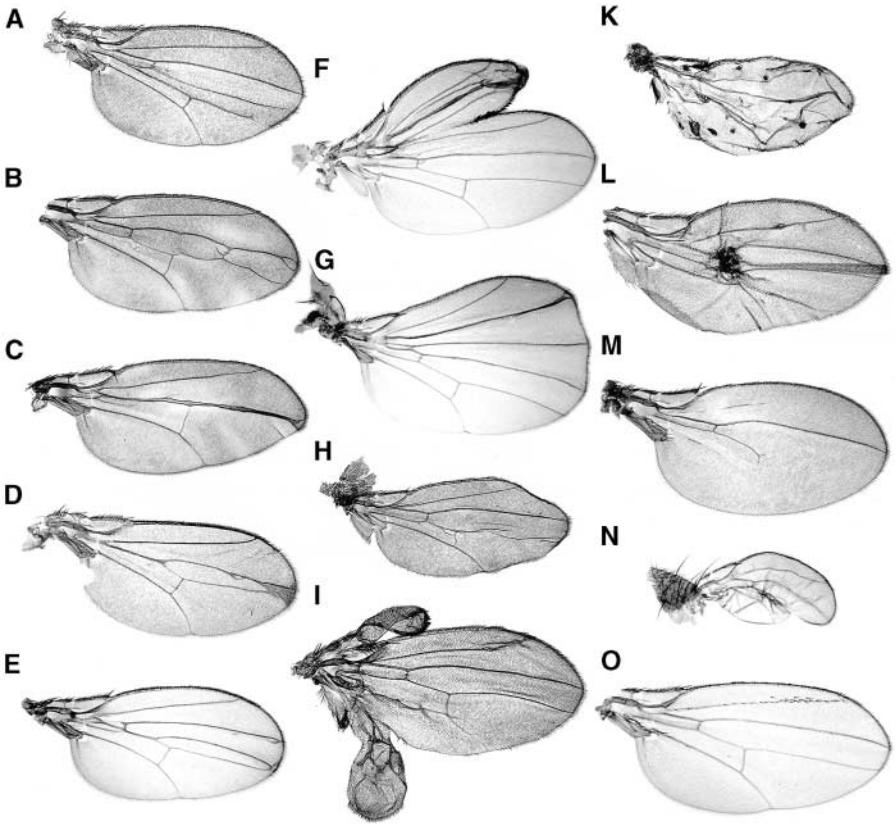

Figure 5.—Representative wings of the complementation groups presented in Table 3. Clones have been induced by *vg::flp*. *smo* (A), *col/kn* (B and C), *fu* (D), new class of *ptc* alleles (E), *pka* (F), *ptc* (G), *en/inv* (H), *brk* (I), *sgg* (K), 2F26 (L), 2D5 (M), 3N5 (N), and 3F43 (O).

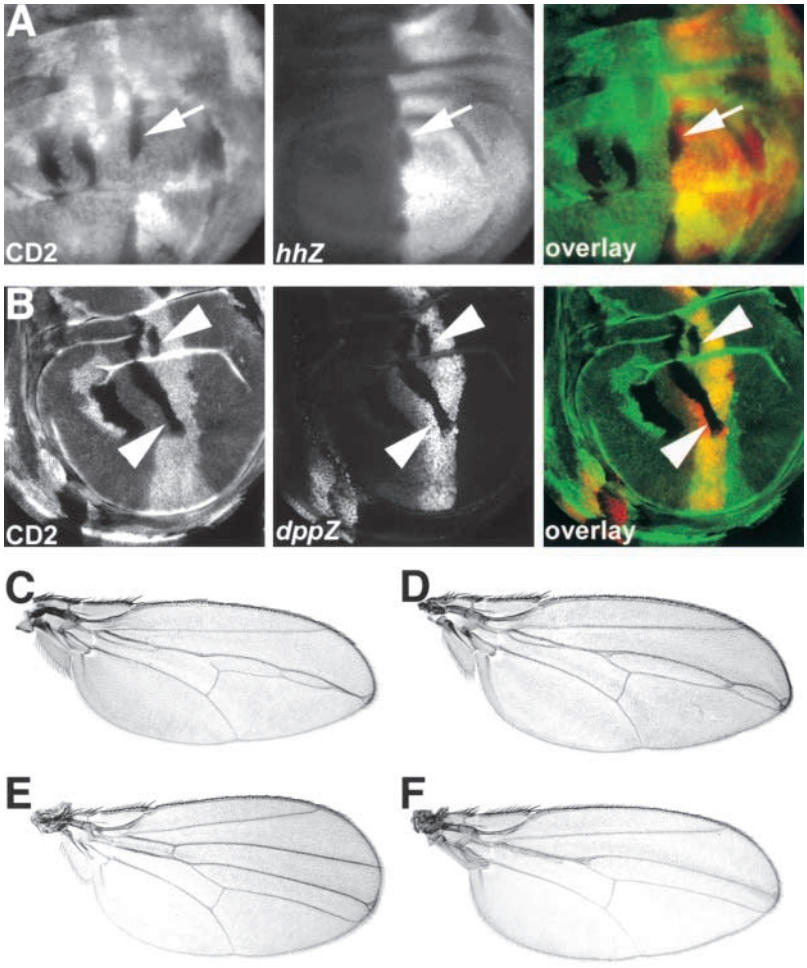

FIGURE 6.—Clones of cells homozygous mutant for the novel class of *ptc* alleles cross the anteroposterior compartment boundary and lose expression of Hh target genes. (A and B) Anterior clones homozygous for the ptc^{P83} allele (marked by the absence of CD2; green in A and B) migrate into territory of the posterior compartment (A; lack of *hhZ* expression in red is marked by arrow) and fail to upregulate the expression of *dppZ* (red in B, arrowhead). The novel *ptc* alleles are partly viable. Wings of the following genotypes are shown: $ptc^{Q67}/Df(2R)44CE$ (C), ptc^{Q67}/ptc^{IIW} (D), $ptc^{Q67}/Df(2R)H3D3$ (E), and $ptc^{P83}/Df(2R)H3D3$ (F).

DISCUSSION

The aim of our screen was to identify genes involved in the formation of the anteroposterior compartment boundary. Specifically, we were interested in finding genes that directly confer A/P compartment-specific cell affinity, and we therefore set up a screen for phenotypes similar to those caused by mutations in *smo*. Cells lacking Smo activity do not exhibit proper A affinity because they cannot respond to Hh. Hence we expected to identify not only putative cell adhesion molecules but also positive regulators of the Hh signaling pathway.

Several screens based on the FRT-FLP method have been successfully implemented for genes affecting wing patterning (JIANG and STRUHL 1995, 1998) and for genes required for integrin-mediated cell adhesion between dorsal and ventral wing surfaces (PROUT *et al.* 1997; WALSH and BROWN 1998). We chose to limit the FLP-induced mosaicism to the wing and found the *vg::flp* transgene combination ideally suited for this. To our surprise and advantage, *vg::flp* activity was not restricted to the region of the D/V boundary. It is possible that the *vg boundary enhancer* is broadly activated by Notch signaling at early stages of wing disc development (K. IRVINE, personal communication).

As a further improvement we generated chromosomes with FRTs flanking both sides of the centromere (2xFRT). The individual FRTs of these chromosomes appear to operate independently of each other, allowing efficient recombination of both chromosomal arms in the same animal. We assumed that the chance of a mutation on one chromosomal arm masking the phenotype caused by a mutation on the other arm would be very low. Indeed, when mutations were retested with single FRT-carrying chromosomes, we found only very few cases where wing phenotypes occurred independently with both arms. An interesting modification of our setup could be to use recessive cell-lethal mutations on both chromosomal arms to eliminate homozygous wild-type cells for one or both arms (NEWSOME *et al.* 2000). We found that 2xFRT chromosomes represent an efficient tool for screens based on the FRT-FLP method.

A total of 250,000 mutant chromosomes covering the X chromosome and both major autosomes were screened. Four complementation groups were identified that af-

TABLE 3

Complementation analysis of the new class of *ptc* alleles

Allelic combination	Viability	% and phenotype of survivors
ptc^{N15}/ptc^{P83}	Lethal	
ptc^{N15}/ptc^{Q67}	Lethal	
ptc^{P83}/ptc^{Q67}	Semilethal	34; thickened L3
Df(2R)44CE/ptc^{N15}	Lethal	
Df(2R)44CE/ptc^{P83}	Lethal	
Df(2R)44CE/ptc^{Q67}	Semilethal	4; L3 and L4 fused
Df(2R)H3D3/ptc^{N15}	Semilethal	14; L3 and L4 fused, slight L3 defects
Df(2R)H3D3/ptc^{P83}	Semilethal	56; thickened L3, ectopic L3
Df(2R)H3D3/ptc^{Q67}	Semilethal	35; thickened L3, ectopic L3
ptc^{Ilw109}/ptc^{N15}	Lethal	
ptc^{Ilw109}/ptc^{P83}	Semilethal	4; L3 and L4 fused
ptc^{Ilw109}/ptc^{Q67}	Semilethal	11; L3 and L4 fused
$ptc^{S2}/ptc^{N15/P83/Q67}$	Viable	
ptc^{Ilw109}/Df(2R)44CE	Lethal	
ptc^{Ilw109}/Df(2R)H3D3	Lethal	
ptc^{S2}/Df(2R)44CE	Lethal	
ptc^{S2}/Df(2R)H3D3	Lethal	
ptc^{S2}/ptc^{Ilw109}	Lethal	

Complementation analysis of the new *ptc* alleles with two deficiencies and two amorphic *ptc* alleles, respectively. Heterozygous combinations that allow fewer animals to survive to adulthood than combinations of fully complementing mutations were designated as semilethal. The extent of semilethality is given as the percentage of expected survivors of a fully complementing allelic combination.

fected wing patterning similar to mutations in *smo*. The largest of these groups represented alleles in *smo* itself. Two groups exhibiting a subset of *smo* phenotypes represented new alleles of *fused* and *collier/knot*. Fused is a positive regulator of Hh signaling, and *collier/knot* is an Hh target gene required for the formation of the L3/L4 intervein region. Surprisingly, the remaining complementation group turned out to consist of novel *ptc* alleles with striking characteristics. Molecularly, they represent point mutations causing an amino acid substitution in either the first or the second large extracellular loop. In contrast to *ptc* null alleles, homozygous mutant clones failed to upregulate Hh target genes even in the presence of Hh. Together these findings suggest that the mutant proteins repress Smo constitutively, most likely because they fail to bind Hh. Animals mutant for *trans*-heterozygous combinations of these new *ptc* alleles with ptc^{S2} were fully viable. The ptc^{S2} product lacks the ability to repress Smo but is able to sequester, and hence bind to, Hh (Chen and Struhl 1996). The intragenic

TABLE 4

Further loci affecting wing patterning

Name	Chromosome/cytology	No. of alleles	Phenotype
pka	II/30C5-7	2	Duplication of L3 up to complete A/P axis duplication
ptc	II/44D2-5	5	Duplication of L3 up to complete A/P axis duplication
cos2	II/50A1-2	1	Duplication of L3 up to complete A/P axis duplication
brk	X/7A4	3	Anterior and posterior wing outgrowths
sgg	X/3B1-2	12	Ectopic margin bristles in the wing blade
2F26	II/2L	6	Massive ectopic veins between L3 and L4 or on L3
2D5	II/2L	1	Homozygous viable with partial up to complete loss of all veins except L3
sos	II/34D1-3	6	Partial loss of L4
cnk	II/54C1	2	Partial loss of L4
XG47	X/?	1	Homo- and hemizygous viable with reduced wing but normal body size
3F43	III/?	2	Ectopic bristles
3N5	III/?	1	Partial loss of P compartment

Selection of complementation groups that gave rise to wing-patterning defects. Cytology according to FlyBase is given where the gene could be confirmed by complementation analysis with a known allele.

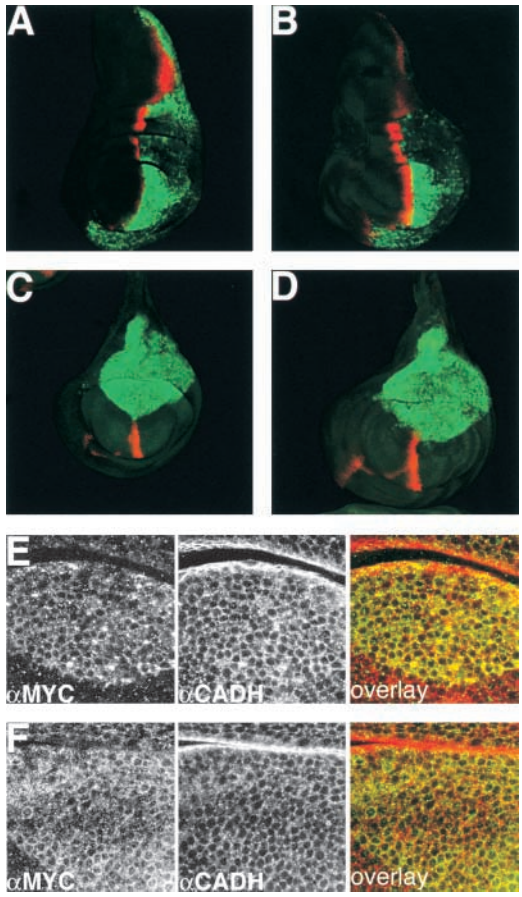

FIGURE 7.—The novel *ptc* alleles fail to sequester Hh but retain the ability to repress Smo. Third instar wing imaginal discs were costained with anti-Myc (green in A–F) and anti-β-Gal (red in A–D) or anti-DE-cadherin (red in E and F), respectively. Wing discs were of the following genotypes: *en-gal4 ptcZ/UAS-ptc^{wt}-myc* (A), *en-gal4 ptcZ/UAS-ptc^{mut}-myc* (B), *apt-gal4 ptcZ/UAS-ptc^{wt}-myc* (C and D), and *apt-gal4 ptcZ/UAS-ptc^{mut}-myc* (E and F).

complementation we observed suggests that both functions of Ptc, binding of Hh and repression of Smo, can be provided by individual proteins that possess only one of each. Recently, it was shown that a combination of two proteins, one consisting of the N- and the other the C-terminal half of Ptc, reconstitutes Ptc function (JOHNSON *et al.* 2000). Although these experiments cannot be directly compared with our findings, together they do suggest that Ptc function can be separated intramolecularly into independent modules of N- *vs.* C-terminal and extra- *vs.* intracellular domains. One possible scenario that could explain the intragenic complementation would be if Ptc proteins act in a multimeric complex.

Besides those genes exhibiting a *smo*-like phenotype, many other mutations that affected the patterning of the wing, as well as its growth, were collected. We identified not only new alleles of most known components of the Hh signaling pathway, but also components of other signal transduction pathways. The vast variety of wing phenotypes observed in this screen suggests that its current setup could be useful to identify other genes involved in distinct processes of wing patterning.

The initial goal of our screen, the identification of a compartment-specific cell affinity gene, was not accomplished. All mutations conferring the phenotype we screened for could be classified as new alleles of known genes. Possible explanations for why no cell affinity genes were found are: the screen did not reach saturation; such genes act redundantly; the phenotype of loss of a compartment-specific cell adhesion molecule differs from that caused by the loss of Hh signaling or En activity; such a gene is essential for cell viability; the model by which transcriptional regulation of a modulator of cell adhesion is responsible for the segregation of A and P cells is incorrect.

Regarding the saturation issue, it must be considered that the entire genome could not be screened. Due to technical limitations, genes proximal to the FRTs and genes on the fourth chromosome are not accessible by the FRT-FLP method. The high number of alleles of certain known genes that we identified indicates that the majority of the genome was screened to saturation. Intriguingly, we found many more complementation groups on the first and second chromosomes compared to those on the third. The spectrum of phenotypes also differed among the chromosomes. Many mutations affecting vein positioning were found on the second chromosome, while the third chromosome revealed a high number of loci affecting growth and size. Uneven distribution of mutations for a specific phenotype, however, is not unusual and was observed in another genome-wide FRT-FLP screen (WALSH and BROWN 1998).

A serious concern is the possibility that the sought-after cell adhesion function is provided by a redundant set of genes. Duplicate genes or the contribution of several loci to the A/P affinity system would prevent the discovery of loss-of-function mutations by our assay. Experimental evidence that overexpression of a single cell adhesion molecule is sufficient to disrupt the A/P compartment boundary (DAHMANN and BASLER 2000) does not rule out this possibility.

It is also possible that the loss of compartment-specific cell affinity would be manifested in phenotypes that differ from those caused by aberrant Hh or En activity. In particular, it is conceivable that the gene coding for the compartment-specific cell adhesion property is essential for the survival of wing cells. Ci and En activities may merely modulate its transcription above a certain threshold required for the segregation of A and P cells. The total loss of this function may cause cell lethality, thereby resulting in a phenotype different from the *smo*-like defects.

In the light of these caveats the outcome of this screen does not rule out the model of differential compartment-specific cell affinity in the establishment of the

lineage restriction boundary. However, within the limits of the saturation discussed above, our results do not support a model in which a single dedicated cell adhesion molecule defines the segregation behavior of A and P cells.

We thank B. Dickson for the FRT40/42 chromosome, G. Struhl for UAS-flp lines, the Bloomington Stock Center for numerous alleles and deficiencies, R. Burke for comments on the manuscript, and the Swiss National Science Foundation and the Kanton of Zürich for support.

LITERATURE CITED

Basler, K., and G. Struhl, 1994 Compartment boundaries and the control of Drosophila limb pattern by hedgehog protein. Nature **368:** 208–214.

Biehs, B., M. A. Sturtevant and E. Bier, 1998 Boundaries in the Drosophila wing imaginal disc organize vein-specific genetic programs. Development **125:** 4245–4257.

Blair, S. S., and A. Ralston, 1997 Smoothened-mediated Hedgehog signalling is required for the maintenance of the anterior-posterior lineage restriction in the developing wing of Drosophila. Development **124:** 4053–4063.

Chen, Y., and G. Struhl, 1996 Dual roles for patched in sequestering and transducing Hedgehog. Cell **87:** 553–563.

Chen, Y., and G. Struhl, 1998 In vivo evidence that Patched and Smoothened constitute distinct binding and transducing components of a Hedgehog receptor complex. Development **125:** 4943–4948.

Dahmann, C., and Basler, K., 1999 Compartment boundaries: at the edge of development. Trends Genet. **15:** 320–326.

Dahmann, C., and Basler, K., 2000 Opposing transcriptional outputs of Hedgehog signaling and engrailed control compartmental cell sorting at the Drosophila A/P boundary. Cell **100:** 411–422.

Garcia-Bellido, A., 1975 Genetic control of wing disc development in Drosophila. Ciba Found. Symp. **0** (29): 161–182.

Garcia-Bellido, A., P. Ripoll and G. Morata, 1973 Developmental compartmentalisation of the wing disk of Drosophila. Nat. New Biol. **245:** 251–253.

Golic, K. G., 1991 Site-specific recombination between homologous chromosomes in Drosophila. Science **252:** 958–961.

Jiang, J., and G. Struhl, 1995 Protein kinase A and hedgehog signaling in Drosophila limb development. Cell **80:** 563–572.

Jiang, J., and G. Struhl, 1998 Regulation of the Hedgehog and Wingless signalling pathways by the F-box/WD40-repeat protein Slimb. Nature **391:** 493–496.

Johnson, R. L., L. Milenkovic and M. P. Scott, 2000 In vivo functions of the patched protein: requirement of the C terminus for target gene inactivation but not Hedgehog sequestration. Mol. Cell **6:** 467–478.

Kim, J., A. Sebring, J. J. Esch, M. E. Kraus, K. Vorwerk *et al.*, 1996 Integration of positional signals and regulation of wing formation and identity by Drosophila vestigial gene. Nature **382:** 133–138.

Lawrence, P. A., and G. Morata, 1976 Compartments in the wing of Drosophila: a study of the engrailed gene. Dev. Biol. **50:** 321–337.

Lawrence, P. A., and G. Struhl, 1996 Morphogens, compartments, and pattern: Lessons from Drosophila? Cell **85:** 951–961.

Lecuit, T., W. J. Brook, M. Ng, M. Calleja, H. Sun *et al.*, 1996 Two distinct mechanisms for long-range patterning by Decapentaplegic in the Drosophila wing. Nature **381:** 387–393.

Martin, V., G. Carrillo, C. Torroja and I. Guerrero, 2001 The sterol-sensing domain of Patched protein seems to control Smoothened activity through Patched vesicular trafficking. Curr. Biol. **11:** 601–607.

Nellen, D., R. Burke, G. Struhl and K. Basler, 1996 Direct and long-range action of a DPP morphogen gradient. Cell **85:** 357–368.

Newsome, T. P., B. Asling and B. J. Dickson, 2000 Analysis of Drosophila photoreceptor axon guidance in eye-specific mosaics. Development **127:** 851–860.

Preat, T., P. Therond, C. Lamour-Isnard, B. Limbourg-Bouchon, H. Tricoire *et al.*, 1990 A putative serine/threonine protein kinase encoded by the segment-polarity fused gene of Drosophila. Nature **347:** 87–89.

Prout, M., Z. Damania, J. Soong, D. Fristrom and J. W. Fristrom, 1997 Autosomal mutations affecting adhesion between wing surfaces in *Drosophila melanogaster*. Genetics **146:** 275–285.

Rodriguez, I., and K. Basler, 1997 Control of compartmental affinity boundaries by hedgehog. Nature **389:** 614–618.

Strutt, H., C. Thomas, Y. Nakano, D. Stark, B. Neave *et al.*, 2001 Mutations in the sterol-sensing domain of Patched suggest a role for vesicular trafficking in Smoothened regulation. Curr. Biol. **11:** 608–613.

Vervoort, M., M. Crozatier, D. Valle and A. Vincent, 1999 The COE transcription factor collier is a mediator of short-range hedgehog-induced patterning of the Drosophila wing. Curr. Biol. **9:** 632–639.

Walsh, E. P., and N. H. Brown, 1998 A screen to identify Drosophila genes required for integrin-mediated adhesion. Genetics **150:** 791–805.

Xu, T., and G. M. Rubin, 1993 Analysis of genetic mosaics in developing and adult Drosophila tissues. Development **117:** 1223–1237.

Communicating editor: K. Golic